

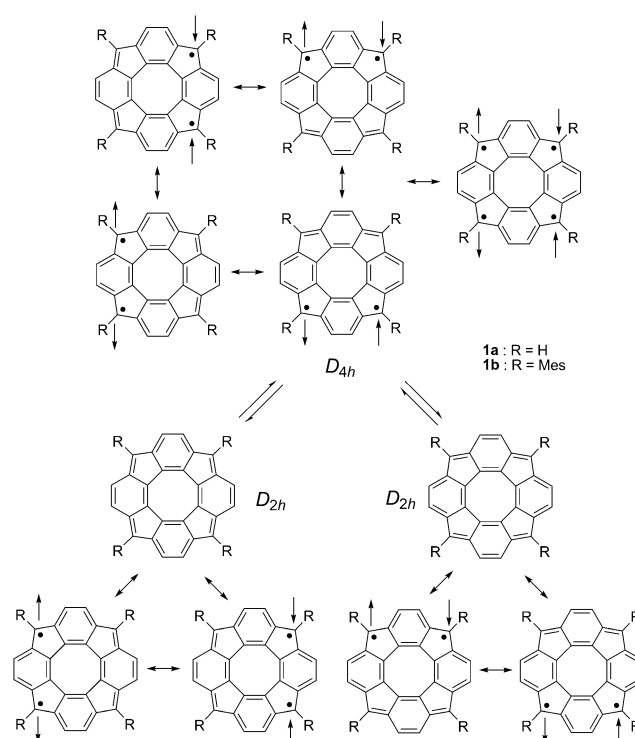
# Tetracyclopenta[def,jkl,pqr,vwx]tetraphenylene: A Potential Tetraradicaloid Hydrocarbon\*\*

Shunpei Nobusue, Hirokazu Miyoshi, Akihiro Shimizu, Ichiro Hisaki, Kotaro Fukuda, Masayoshi Nakano, and Yoshito Tobe\*

**Abstract:** A tetramesityl derivative of hitherto unknown tetracyclopenta[def,jkl,pqr,vwx]tetraphenylene (TCPTP), which is a potential tetraradicaloid hydrocarbon, was synthesized. Theoretical calculations based on spin-flip time-dependent density functional theory predict that the closed-shell  $D_{2h}$  form of TCPTP is more stable than the open-shell  $D_{4h}$  form with its slightly tetraradical character. The tetramesityl derivative ( $Mes$ )<sub>4</sub>-TCPTP exhibits remarkable antiaromaticity as a result of the peripheral 20- $\pi$ -electron circuit, which causes an absorption maximum at a long wavelength and a small HOMO–LUMO gap. In solution, ( $Mes$ )<sub>4</sub>-TCPTP most likely adopts rapidly equilibrating  $D_{2h}$  structures that interconvert via the  $D_{4h}$  transition state. X-ray crystallographic analysis showed ( $Mes$ )<sub>4</sub>-TCPTP as an approximate  $D_{2h}$  structure.

We report the synthesis, structure, and fundamental physical properties of compound **1b**, a tetramesityl derivative of hitherto unknown tetracyclopenta[def,jkl,pqr,vwx]tetraphenylene (TCPTP, **1a**). Particularly noteworthy aspects of compound **1a** include:

- 1) Closed-shell  $D_{2h}$  and open-shell  $D_{4h}$  structures exist, and their mutual interconversion (Scheme 1) is similar to that observed for cyclobutadiene (CBD). For CBD, the valence tautomerization that interconverts the two rec-



**Scheme 1.** Valence tautomerization of **1a** and **1b** with closed-shell  $D_{2h}$  isomers (bottom) with a small diradical character via a  $D_{4h}$  isomer (top) with open-shell diradical and tetraradical characters.

tangular  $D_{2h}$  isomers via the square  $D_{4h}$  transition state of diradical character has been the topic of controversy for more than thirty years, even after numerous experimental and theoretical investigations have been done.<sup>[1,2]</sup>

- 2) **1a** contains 28  $\pi$  electrons distributed over an inner 8- $\pi$ -electron system and an outer 20- $\pi$ -electron system, both of which can be antiaromatic in their highest symmetry forms. The inner 8- $\pi$ -electron system is fixed in a planar geometry and has relevance to planar cyclooctatetraenes (COTs), which also attracted substantial interest from synthetic and theoretical chemists.<sup>[3]</sup> For example, a few derivatives were synthesized in which a COT core was forced to adopt a planar geometry.<sup>[3]</sup> Moreover, the  $D_{8h}$  transition state of the bond shifting between  $D_{4h}$  COTs

[\*] Dr. S. Nobusue,<sup>[†]</sup> H. Miyoshi, Dr. A. Shimizu,<sup>[‡]</sup> Prof. Y. Tobe  
Division of Frontier Materials Science  
Graduate School of Engineering Science, Osaka University  
1-3 Machikaneyama, Toyonaka, Osaka 560-8531 (Japan)  
E-mail: tobe@chem.es.osaka-u.ac.jp

K. Fukuda, Prof. M. Nakano  
Department of Materials Engineering Science  
Graduate School of Engineering Science, Osaka University  
Osaka (Japan)

Dr. I. Hisaki  
Department of Material and Life Science  
Graduate School of Engineering, Osaka University  
Osaka (Japan)

[†] Present address: Department of Chemistry  
Graduate School of Science, Nagoya University  
Nagoya (Japan)

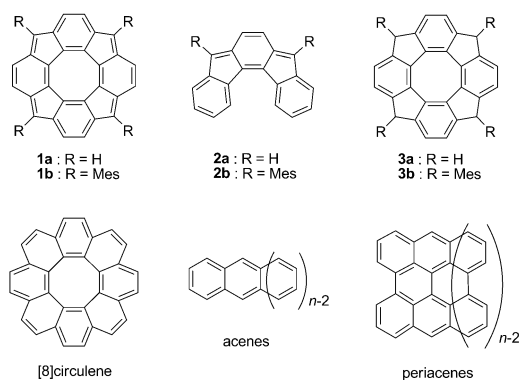
[‡] Present address: Department of Synthetic and Biological Chemistry,  
Graduate School of Engineering, Kyoto University  
Kyoto (Japan)

[\*\*] This work was supported by Grants-in-Aid for Scientific Research from the Ministry of Education, Culture, Sports, Science and Technology (Japan). The authors acknowledge Prof. T. Kubo of Osaka University (Japan) for the use of facilities and valuable discussions. The synchrotron radiation experiments were performed at the BL38B1 of SPring-8 with the approval of the Japan Synchrotron Radiation Research Institute (JASRI; proposal No. 2013B1245, 2014A1252). The authors are grateful to Dr. S. Baba and Dr. N. Mizuno for crystallographic data collection.

Supporting information for this article is available on the WWW under <http://dx.doi.org/10.1002/anie.201410791>.

was experimentally shown to violate the Hund's rule in a strictest sense.<sup>[4]</sup>

- 3) **1a** is a cyclic congener of indeno[2,1-*c*]fluorene (**2a**),<sup>[5]</sup> one of the indenofluorene isomers, which have attracted keen interest because of their semiconducting character, resulting from small band gaps, and their nonlinear optical properties, arising from their singlet diradical characters.<sup>[6,7]</sup> It should be emphasized that **1a** represents a potential singlet tetraradicaloid compound with a hydrocarbon framework (Scheme 1, the top right canonical structure). A stable tetraradical consisting of two diboradiphosphinocyclobutane rings linked by a *meta*-phenylene has been reported previously.<sup>[8]</sup> Although large polycyclic aromatic hydrocarbons, such as an acene with 20 rings (icosacene:  $n = 20$ ) and periacenes with more than 8 zigzag-edge rings (perioctacene,  $n = 8$ ), are expected to have tetraradical ground states, such materials have not yet been prepared.<sup>[9]</sup>
- 4) Compound **1a** can be regarded as a member of the corannulene family, according to the corannulene concept proposed by Hellwinkel,<sup>[10]</sup> and as a smaller analogue of [8]circulene, whose derivatives, including its tetrabenzo homologues, have been prepared recently.<sup>[11]</sup> Although Hellwinkel and Reiff reported the generation of a dicationic species of **1a** (with 26  $\pi$  electrons) from its tetrahydro derivative **3a** in a mass spectrometry sample chamber,<sup>[12]</sup> isolation and characterization of **1a** or its derivatives have not been reported.



Herein we report the theoretical investigation of the relationship between the open-shell singlet character and the structures of these compounds. The optimized geometries of these antiaromatic molecules, which are composed of five- and six-membered rings, often depend significantly on the calculation methods, as shown for *s*-indacene.<sup>[13]</sup> We thus applied the unrestricted natural orbital complete active space method,<sup>[14]</sup> UNO-CAS(4,4)/6-311G(d,p), and the spin-flip time-dependent density functional theory (SF-TD-BHHLYP/6-311G(d,p)) methods, which reproduced the experimental structures of such molecules very well.<sup>[15]</sup> These two methods provided similar structures for the present systems (Figure S12 and S13), so that the geometries optimized with SF-TD-BHHLYP/6-311G(d,p) were employed for later discussion. We first investigated the diradical characters,

which are determined by the occupation numbers  $y_0$  and  $y_1$  of the lowest and second lowest unoccupied natural orbital (LUNO and LUNO + 1, respectively). These were obtained by the long-range-corrected LC-UBLYP/6-311 + G(d,p) method,<sup>[16]</sup> which is known to semiquantitatively reproduce the open-shell characters obtained by highly-electron-correlated methods.<sup>[17]</sup> The  $y_0$  and  $y_1$  values ranged from 0 to 1 ( $y_0 \geq y_1$ ), thus indicating the diradical and tetraradical characters, that is,  $(y_0, y_1) = (1, 0)$  indicates a purely diradical character, while  $(y_0, y_1) = (1, 1)$  indicates a purely tetraradical character.

Table 1 lists the calculated  $y_0$  and  $y_1$  values for three model systems, that is, model A (with the structure of **1a** optimized under the constraint of  $D_{2h}$  symmetry) and model B (with the

**Table 1:** Occupation numbers  $y_0$  and  $y_1$  of the lowest and second lowest unoccupied natural orbitals (LUNO and LUNO + 1, respectively) obtained by LC-UBLYP/6-311 + G(d,p) for models A–C of **1a**.

Occupation number	Model A	Model B	Model C
$y_0$	0.095	1.000	0.258
$y_1$	0.032	0.166	0.085

structure of **1a** optimized under the constraint of  $D_{4h}$  symmetry). We also examined model C with the structure of the TCPTP part of **1b** experimentally obtained by X-ray crystallographic analysis (described below). Table 2 shows the bond lengths of the peripheral bonds  $a$ – $j$ , internal bonds  $k$ – $n$ , and spoke bonds  $o$ – $r$  of models A–C (Figure 1). The structure of the  $D_{2h}$  symmetric model A is similar to that of the experimental model C (Table 2, and Figure S12 in the Supporting Information) and shows a relatively small diradical character ( $y_0 = 0.095$  for model A and 0.258 for model C). On the other hand, the  $D_{4h}$  symmetric model B, which had a higher energy (34.7 kJ mol<sup>−1</sup> at the SF-TD-BHHLYP/6-311G(d,p) level of approximation) than model A, featured a significant  $y_0$  value (1.000) together with a small  $y_1$  value

**Table 2:** Calculated (models A and B) and experimental (model C) bond lengths for the TCPTP core.

Bond <sup>[a]</sup>	Model A <sup>[b]</sup>	Model B <sup>[b]</sup>	Model C <sup>[c]</sup>
<i>a</i>	1.447	1.397	1.460(6)
<i>b</i>	1.350	1.397	1.371(6)
<i>c</i>	1.437	1.403	1.433(6)
<i>d</i>	1.339	1.366	1.349(6)
<i>e</i>	1.437	1.403	1.440(5)
<i>f</i>	1.350	1.397	1.373(5)
<i>g</i>	1.447	1.397	1.452(6)
<i>h</i>	1.378	1.403	1.391(6)
<i>i</i>	1.390	1.366	1.390(6)
<i>j</i>	1.378	1.403	1.380(6)
<i>k</i>	1.476	1.477	1.479(5)
<i>l</i>	1.344	1.359	1.359(5)
<i>m</i>	1.476	1.477	1.487(5)
<i>n</i>	1.373	1.359	1.379(6)
<i>o</i>	1.469	1.442	1.481(5)
<i>p</i>	1.469	1.442	1.476(6)
<i>q</i>	1.420	1.442	1.433(5)
<i>r</i>	1.420	1.442	1.435(5)

[a] Bond positions are shown in Figure 1. [b] Calculated at the SF-TD-BHHLYP/6-311G(d,p) level. [c] Data obtained from X-ray analysis of **1b**.

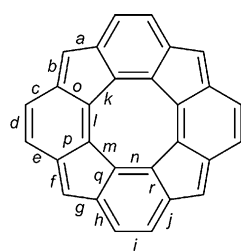


**Figure 1.** Bond numbering for models A–C of **1a**.

(0.166). The relationship between the open-shell characters and the structures can be explained with the resonance structures for closed-shell ( $D_{2h}$  symmetric), diradical ( $C_{2v}$  symmetric), and tetraradical ( $D_{4h}$  symmetric) forms (Scheme 1). Indeed, the bond-length alternation (BLA) for the outer-ring region (bonds  $a$ – $j$  in Figure 1) is reduced in model B compared with models A and C (Figure S12). This alteration coincides with that observed in the diradical and tetraradical resonance structures (Scheme 1). These results indicate that the  $D_{2h}$  structure exhibits a slightly diradical nature, while the  $D_{4h}$  structure exhibits a significantly diradical nature together with a slightly tetraradical nature. In order to investigate the spatial contribution of unpaired electrons to the diradical characters, we calculated the odd-electron-density distributions for models B and C (Figure 2),<sup>[17]</sup> which are divided into contributions from  $y_0$

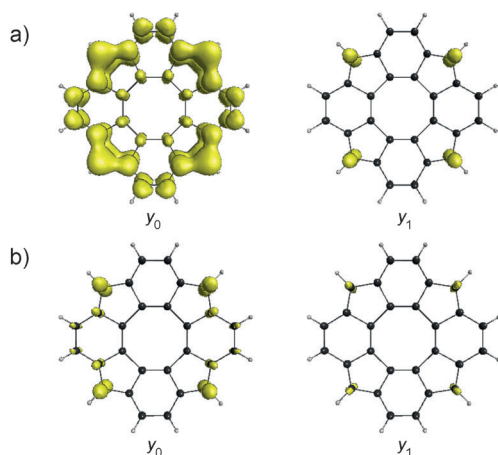
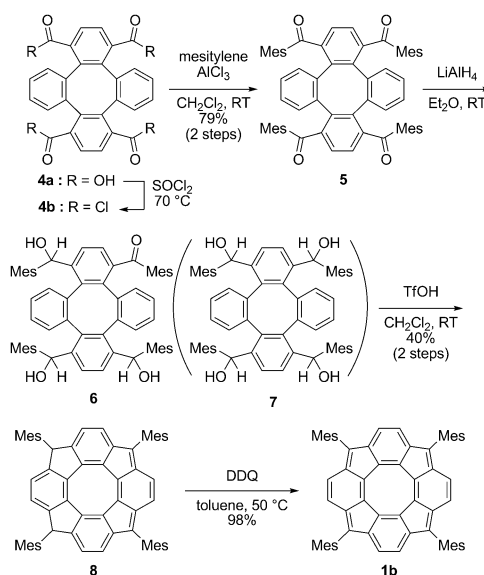


**Figure 2.** Odd-electron-density distributions of  $y_0$  and  $y_1$  of models B (a) and C (b) calculated at the LC-UBLYP/6-311 + G(d,p) level [contour value of 0.0025 a.u.; 1 a.u. = 27.21 eV].

and  $y_1$ . The odd-electron densities of  $y_0$  have much larger amplitudes than those of  $y_1$ . Moreover, their distributions are largest on the carbon atoms in the five-membered rings for both  $y_0$  and  $y_1$ , which can be explained with the diradical and tetraradical resonance structures (Scheme 1).

We started the synthesis of **1b** from the known tetracarboxylic acid **4a**<sup>[18]</sup> (Scheme 2). A Friedel–Crafts reaction of acid chloride **4b** with mesitylene gave tetraketone **5**. After treatment of **5** with  $\text{LiAlH}_4$ , the crude product was subjected without purification to an intramolecular alkylation by treatment with trifluoromethanesulfonic acid. However, the product of the alkylation was not the expected tetrahydro derivative **3b**, but dihydro-TCPTP **8**. We assumed that the reduction of **5** was not complete because of the low solubility of the alkoxide intermediates, which precipitated out from the reaction mixture, giving triol **6** instead of tetraol **7**.<sup>[19]</sup>



**Scheme 2.** Synthesis of **1b**.

Dehydrogenation of **8** with DDQ gave product **1b** as a dark brown solid that was stable in air for at least a few months.

The  $^1\text{H}$  NMR spectrum of **1b** measured in  $[\text{D}_8]\text{toluene}$  at  $30^\circ\text{C}$  exhibits a singlet at 2.85 ppm for the core “aromatic” proton (Figure S3), which is remarkably upfield shifted compared to the corresponding proton of hemicircular hydrocarbon **2b**<sup>[5]</sup> and dihydro derivative **8** (6.13 and 5.84 ppm in  $\text{CDCl}_3$ , respectively). The nucleus-independent chemical shift (NICS(1)) values (LC-UBLYP/6-311 + G(d,p)) calculated for the observed TCPTP core (model C) and  $D_{2h}$  symmetric **1a** (model A) indicate that the six-membered rings are either weakly aromatic or antiaromatic (Figure 3), thus suggesting that the “aromatic” proton would exhibit an averaged chemical shift in a nonaromatic region. The remarkable upfield shift is therefore ascribed to the paramagnetic shielding effect of the outer  $20\text{-}\pi$ -electron system. At higher temperatures ( $50^\circ\text{C}$ ), the signals start to broaden, thus indicating the population of the thermally excited triplet state (Figure S4). Theoretically estimated vertical singlet–triplet energy gaps (81 and  $69\text{ kJ mol}^{-1}$  for models A and C, respectively) at the SF-TD-PBE0/6-311G(d,p) level of theory,<sup>[20]</sup> are however relatively large. The appearance of a single signal for the core proton indicates that **1b** adopts the

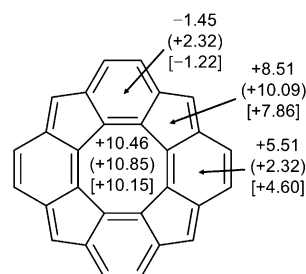


**Figure 3.** NICS(1) values of **1a** in models A, B (in round brackets), and C [in square brackets] calculated at the LC-UBLYP/6-311 + G(d,p) level.

$D_{4h}$  structure or exists in a rapid equilibrium between the  $D_{2h}$  structures. However, no peak separation was observed when the solution was cooled to  $-80^\circ\text{C}$  (Figure S5). Similarly, the  $^{13}\text{C}$  NMR spectrum showed the four signals that were expected for the TCPTP core carbon atoms of  $D_{4h}$  symmetric **1b** at  $30^\circ\text{C}$  (Figure S6). Cooling to  $-60^\circ\text{C}$  barely showed line broadening indicating that the rates of conversion between the  $D_{2h}$  structures became slow on the NMR time scale (Scheme 1). Based on the calculated chemical shifts for the peripheral protons of **1a** (4.86 and 5.38 ppm) by the LC-UBLYP method for the  $D_{2h}$  structure, the energy barrier for the  $D_{2h} \rightleftharpoons D_{2h}$  valence tautomerization is estimated to be smaller than around  $10\text{ kJ mol}^{-1}$ , which is substantially smaller than the theoretically estimated value ( $34.7\text{ kJ mol}^{-1}$ ).

Crystals suitable for X-ray structure analysis were obtained by recrystallization from chloroform.<sup>[21]</sup> As shown in Figure 4, the TCPTP core of **1b** adopts a planar geometry

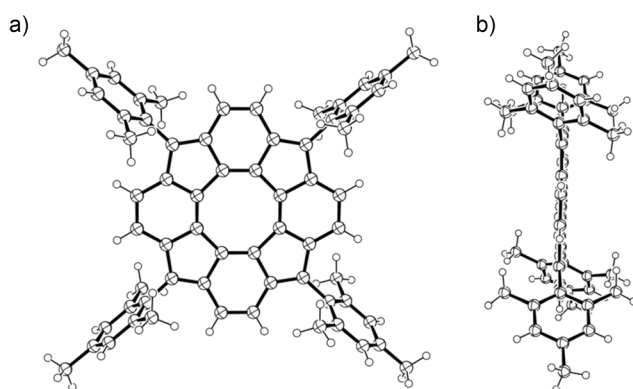


**Figure 4.** a) Top-view and b) side-view ORTEP drawings of **1b** at the 50% probability level. Disordered solvent molecules are omitted for clarity.

with deviations from the mean square plane of less than  $0.0034\text{ \AA}$ . The mesityl groups are oriented nearly perpendicular to the TCPTP plane with dihedral angles of  $72.3\text{--}88.3^\circ$ . The most important feature of the structure of **1b** is that it adopts an approximate  $D_{2h}$  structure, which is evident from the presence of a crystallographic center of inversion. The observed bond lengths at the TCPTP core (model C) are listed in Table 2 together with those of theoretically optimized  $D_{2h}$  model A and  $D_{4h}$  model B. The relatively short bonds *b* ( $1.371\text{ \AA}$ ), *d* ( $1.349\text{ \AA}$ ), *f* ( $1.373\text{ \AA}$ ), and *l* ( $1.359\text{ \AA}$ ), and relatively long bonds *a* ( $1.460\text{ \AA}$ ), *c* ( $1.433\text{ \AA}$ ), *e* ( $1.440\text{ \AA}$ ), and *g* ( $1.452\text{ \AA}$ ) indicate the presence of a *p*-quinodimethane substructure. On the other hand, the bonds *h*, *i*, *j*, and *n* in the other six-membered ring are more homogeneous ( $1.379\text{--}1.391\text{ \AA}$ ), thus suggesting its benzenoid structure. The inner COT ring adopts an approximate  $D_{2h}$  structure with remarkable bond-length alternation: bonds *l* ( $1.359\text{ \AA}$ ) and *n* ( $1.379\text{ \AA}$ ), which are part of the six-membered rings, are shorter than bonds *k* ( $1.479\text{ \AA}$ ) and *m* ( $1.487\text{ \AA}$ ), which are part of the five-membered rings. The data in Table 2 show again that the present SF-TD-DFT calculations at the BHHLYP/6-311G(d,p) level of theory reasonably reproduce the structure of **1b**.

Figure 5 shows UV-Vis-NIR spectra of **1b** and its dihydro derivative **8**. Compound **1b** exhibits an intense absorption maximum at  $475\text{ nm}$  ( $\epsilon = 10100\text{ M}^{-1}\text{ cm}^{-1}$ ) together with a broad band centered at  $909\text{ nm}$  ( $\epsilon = 1210\text{ M}^{-1}\text{ cm}^{-1}$ ) with

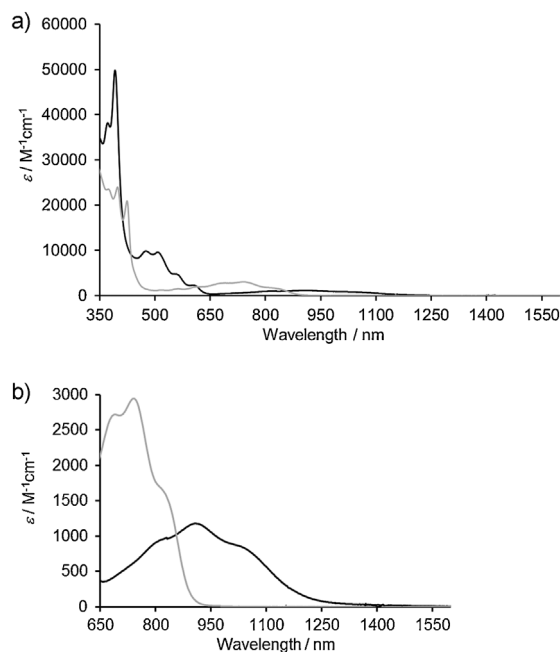


**Figure 5.** a) UV-Vis-NIR spectra of **1b** (black) and dihydro derivative **8** (gray) in  $\text{CH}_2\text{Cl}_2$ . b) NIR region with expanded longitudinal axis.

a low oscillator strength. The lowest energy absorption band is shifted to much longer wavelengths compared to indeno[2,1-*c*]fluorene derivative **2b** ( $\lambda_{\text{max}} = 603\text{ nm}$ )<sup>[5]</sup> and dihydro derivative **8** ( $\lambda_{\text{max}} = 740\text{ nm}$ ) because of the extended conjugation. Time-dependent density functional theory calculations<sup>[22]</sup> (TD-UB3LYP/6-311 + G(d,p) level; Tables S1 and S2) indicate the lowest energy band for model A at  $1079\text{ nm}$  ( $f = 0.0053$ ). The small HOMO–LUMO gap of **1b** was also characterized by cyclic voltammetry and exhibited two reversible oxidation and reduction waves ( $E_1^{\text{ox}} = +0.08$ ,  $E_2^{\text{ox}} = +0.47$ ,  $E_1^{\text{red}} = -1.39$ , and  $E_2^{\text{red}} = -1.68\text{ V}$  vs.  $\text{Fc}/\text{Fc}^+$ , see Figure S11 in Supporting Information).

In conclusion, we succeeded in the synthesis of a tetramesityl derivative (**1b**) of hitherto unknown tetracyclopenta[*defjklpqr,vwx*]tetraphenylene (**1a**). Regarding its molecular structure, that is, an open-shell  $D_{4h}$  or a closed-shell  $D_{2h}$  structure, results of an NMR study suggested the existence of **1b** as rapidly equilibrating  $D_{2h}$  structures through valence tautomerization in solution. In crystals containing a chloroform solvate molecule, it adopts an approximate  $D_{2h}$  structure. Studies are under way to force **1b** and other derivatives of **1a** to adopt the  $D_{4h}$  structure by establishing electronic and/or steric perturbations arising from external factors, including substituents.<sup>[23]</sup>

Received: November 5, 2014

Published online: January 14, 2015



**Keywords:** antiaromaticity · corannulenes · singlet diradical · singlet tetraradical · valence tautomerization

- [1] For reviews of earlier works, see: a) T. Bally, S. Masamune, *Tetrahedron* **1980**, *36*, 343–370; b) G. Maier, *Angew. Chem. Int. Ed. Engl.* **1988**, *27*, 309–332; *Angew. Chem.* **1988**, *100*, 317–341; c) B. R. Arnold, J. Michl, in *Kinetics and Spectroscopy of Carbenes and Biradicals* (Ed.: M. S. Platz), Plenum, New York, **1990**, pp. 1–35.
- [2] See for example: a) B. R. Arnold, J. Michl, *J. Phys. Chem.* **1993**, *97*, 13348–13354; b) M. Eckert-Maksić, M. Vazdar, M. Barbatti, H. Lischka, Z. B. Maksić, *J. Chem. Phys.* **2006**, *125*, 064310; c) T. Saito, S. Nishihara, Y. Kitagawa, T. Kawakami, S. Yamanaka, M. Okumura, K. Yamaguchi, *Chem. Phys. Lett.* **2010**, *498*, 253–258.
- [3] a) K. K. Baldrige, J. S. Siegel, *J. Am. Chem. Soc.* **2001**, *123*, 1755–1759; b) A. Matsuura, K. Komatsu, *J. Am. Chem. Soc.* **2001**, *123*, 1768–1769; c) Y. Nakamura, N. Aratani, H. Shinokubo, A. Takagi, T. Kawai, T. Matsumoto, Z. S. Yoon, D. Y. Kim, T. K. Ahn, D. Kim, A. Muranaka, N. Kobayashi, A. Osuka, *J. Am. Chem. Soc.* **2006**, *128*, 4119–4127; for reviews: d) J. F. M. Oth, *Pure Appl. Chem.* **1971**, *25*, 573–622; e) T. Nishinaga, T. Ohmae, M. Iyoda, *Symmetry* **2010**, *2*, 76–97.
- [4] P. G. Wenthold, D. A. Hrovat, W. T. Borden, W. C. Lineberger, *Science* **1996**, *272*, 1456–1459.
- [5] A. G. Fix, P. E. Deal, C. L. Vonnegut, B. D. Rose, L. N. Zakharov, M. M. Haley, *Org. Lett.* **2013**, *15*, 1362–1365.
- [6] a) D. T. Chase, B. D. Rose, S. P. McClintock, L. N. Zakharov, M. M. Haley, *Angew. Chem. Int. Ed.* **2011**, *50*, 1127–1130; *Angew. Chem.* **2011**, *123*, 1159–1162; b) D. T. Chase, A. G. Fix, S. J. Kang, B. D. Rose, C. D. Weber, Y. Zhong, L. N. Zakharov, M. C. Lonergan, C. Nuckolls, M. M. Haley, *J. Am. Chem. Soc.* **2012**, *134*, 10349–10352; c) A. Shimizu, Y. Tobe, *Angew. Chem. Int. Ed.* **2011**, *50*, 6906–6910; *Angew. Chem.* **2011**, *123*, 7038–7042; d) A. Shimizu, R. Kishi, M. Nakano, D. Shiomi, K. Sato, T. Takui, I. Hisaki, M. Miyata, Y. Tobe, *Angew. Chem. Int. Ed.* **2013**, *52*, 6076–6079; *Angew. Chem.* **2013**, *125*, 6192–6195; for recent reviews, see: e) A. G. Fix, D. T. Chase, M. M. Haley, *Top. Curr. Chem.* **2014**, *349*, 159–195; f) A. Shimizu, S. Nobusue, H. Miyoshi, Y. Tobe, *Pure Appl. Chem.* **2014**, *86*, 517–528.
- [7] For recent reviews on singlet diradical hydrocarbons, see: a) Z. Sun, Q. Ye, C. Chi, J. Wu, *Chem. Soc. Rev.* **2012**, *41*, 7857–7889; b) M. Abe, *Chem. Rev.* **2013**, *113*, 7011–7088; c) Z. Sun, Z. Zeng, J. Wu, *Acc. Chem. Res.* **2014**, *47*, 2582–2591; d) Z. Sun, J. Wu, *Top. Curr. Chem.* **2014**, *349*, 197–248; e) T. Kubo, *Chem. Lett.* **2014**, DOI: 10.1246/cl.140997.
- [8] A. Rodriguez, F. S. Tham, W. W. Schoeller, G. Bertrand, *Angew. Chem. Int. Ed.* **2004**, *43*, 4876–4880; *Angew. Chem.* **2004**, *116*, 4984–4988.
- [9] a) D. Jiang, S. Dai, *J. Phys. Chem. A* **2008**, *112*, 332–335; b) W. Mizukami, Y. Kurashige, T. Yanai, *J. Chem. Theory Comput.* **2013**, *9*, 401–407.
- [10] According to the corannulene concept, corannulenes are defined as compounds possessing an inner annulene system that is connected through all its radial valences with an outer annulene system. Using this nomenclature, **1a** is named [8,20<sup>2,1,2,1,2,1,2,1</sup>]corannulene: D. Hellwinkel, *Chem.-Ztg.* **1970**, *94*, 715–718.
- [11] a) C.-N. Feng, M.-Y. Kuo, Y.-T. Wu, *Angew. Chem. Int. Ed.* **2013**, *52*, 7791–7794; *Angew. Chem.* **2013**, *125*, 7945–7948; b) Y. Sakamoto, T. Suzuki, *J. Am. Chem. Soc.* **2013**, *135*, 14074–14077; c) R. W. Miller, A. K. Duncan, S. T. Schneebeli, D. L. Gray, A. C. Whalley, *Chem. Eur. J.* **2014**, *20*, 3705–3711.
- [12] D. Hellwinkel, G. Reiff, *Angew. Chem. Int. Ed. Engl.* **1970**, *9*, 527–528; *Angew. Chem.* **1970**, *82*, 516–517.
- [13] a) R. H. Hertwig, M. C. Holthausen, W. Koch, Z. B. Maksić, *Angew. Chem. Int. Ed. Engl.* **1994**, *33*, 1192–1194; *Angew. Chem.* **1994**, *106*, 1252–1254; b) M. Nendel, B. Goldfuss, K. N. Houk, K. Hafner, *J. Mol. Chem. Struct. (THEOCHEM)* **1999**, *461–462*, 23–28.
- [14] a) K. Yamaguchi, *Int. J. Quantum. Chem. Symp.* **1980**, *18*, 269–284; b) J. M. Bofill, P. Pulay, *J. Chem. Phys.* **1989**, *90*, 3637–3646.
- [15] R. Kishi, M. Nakano, S. Ohta, A. Takebe, M. Nate, H. Takahashi, T. Kubo, K. Kamada, K. Ohta, B. Champagne, E. Botek, *J. Chem. Theory Comput.* **2007**, *3*, 1699–1707.
- [16] H. Iikura, T. Tsuneda, T. Yanai, K. Hirao, *J. Chem. Phys.* **2001**, *115*, 3540–3544.
- [17] M. Nakano, H. Fukui, T. Minami, K. Yoneda, Y. Shigeta, R. Kishi, B. Champagne, E. Botek, T. Kubo, K. Ohta, K. Kamada, *Theor. Chem. Acc.* **2011**, *130*, 711–724; Erratum: M. Nakano, H. Fukui, T. Minami, K. Yoneda, Y. Shigeta, R. Kishi, B. Champagne, E. Botek, T. Kubo, K. Ohta, K. Kamada, *Theor. Chem. Acc.* **2011**, *130*, 725.
- [18] D. Hellwinkel, G. Reiff, V. Nykodym, *Justus Liebigs Ann. Chem.* **1977**, 1013–1025.
- [19] We are grateful to Prof. Dietmar Kuck (University of Bielefeld) for pointing out this possibility.
- [20] Y. A. Bernard, Y. Shao, A. I. Krylov, *J. Chem. Phys.* **2012**, *136*, 204103.
- [21] CCDC-1016787 (**1b**) contains the supplementary crystallographic data for this paper. These data can be obtained free of charge from The Cambridge Crystallographic Data Centre via [www.ccdc.cam.ac.uk/data\\_request/cif](http://www.ccdc.cam.ac.uk/data_request/cif).
- [22] a) E. Runge, E. K. U. Gross, *Phys. Rev. Lett.* **1984**, *52*, 997–1000; b) E. K. U. Gross, W. Kohn, *Adv. Quant. Chem.* **1990**, *21*, 255–291.
- [23] For example, tetra-*tert*-butyl-*s*-indacene was reported to adopt an approximate  $D_{2h}$  structure in crystals. This structure is a transition-state of valence tautomerization of  $C_{2h}$ -symmetric isomers: J. D. Dunitz, C. Krüger, H. Irngartinger, E. F. Maverick, Y. Wang, M. Nixdorf, *Angew. Chem. Int. Ed. Engl.* **1988**, *27*, 387–389; *Angew. Chem.* **1988**, *100*, 415–418.